Plant Physiology and Biochemistry 237 (2026) 111517

Contents lists available at ScienceDirect

Plant Physiology and Biochemistry

journal homepage: www.elsevier.com/locate/plaphy

Morpho-anatomical and biochemical plasticity of chia (*Salvia hispanica* L.) microgreens following heavy-ion seed irradiation

Sara De Francesco [a,*], Chiara Amitrano [a], Ermenegilda Vitale [b], Walter Tinganelli [c], Marco Durante [c,d], Stefania De Pascale [a], Carmen Arena [b], Veronica De Micco [a,**]

[a] Department of Agricultural Sciences, University of Naples Federico II, Portici, Naples, 80055, Italy
[b] Department of Biology, University of Naples Federico II, Naples, 80126, Italy
[c] GSI Helmholtzzentrum für Schwerionenforschung GmbH, Biophysics Department, Planckstraße 1, Darmstadt, 64291, Germany
[d] Department of Physics "E. Pancini", University of Naples Federico II, Naples, 80126, Italy

ARTICLE INFO

Keywords:
Salvia hispanica L.
Extreme environments
Ionizing radiation
Radiobiology
Stress response
Phenotypic plasticity
Physiological plasticity
Biochemical responses

ABSTRACT

Salvia hispanica L. (chia) microgreens are recognized as nutrient-dense crops suitable for controlled-environment agriculture but never been tested for space-related applications. Elucidating the physiological and biochemical responses of plants to ionizing radiation is essential for crop selection in space agriculture. Ground-based studies, employing irradiation of seeds with heavy ions as components of Galactic Cosmic Rays, are needed to identify radiation-tolerant crops suitable for long-duration missions. This study aimed to evaluate the effects of carbon (^{12}C) and iron (^{56}Fe) ions, on the morphological, anatomical, and biochemical traits of chia microgreens, as a candidate, emerging crop, for space cultivation. Dry seeds were irradiated with five doses (0.3, 1, 10, 20, and 25 Gy) of each ion type, and responses were assessed at the seedling stage. Distinct ion-specific and dose-dependent responses were observed across multiple functional traits. Iron irradiation promoted shoot elongation, photosynthetic pigment and soluble protein contents, whereas carbon ions increased seedling transpiration, nutrient accumulation (K, Mg, Ca), and polyphenol content, accompanied by notable anatomical adjustments in leaf tissues. Despite these structural and biochemical adjustments, net photosynthesis remained unaffected by irradiation treatments. However, P_N contributed to sample separation in the PCA through its covariation with other morpho-physiological and biochemical traits. Phenotypic plasticity analysis revealed higher responsiveness of biochemical traits than anatomical ones, particularly under iron ion exposure. Overall, the ability of *S. hispanica* microgreens to preserve photosynthetic performance, while modulating key functional traits under ionizing radiation, underscores their physiological plasticity and provides evidence supporting their potential suitability for space-based cultivation systems.

1. Introduction

Salvia hispanica L., commonly known as chia, is a flowering plant belonging to the Lamiaceae family, native to Central America. Historically consumed by ancient Mesoamerican civilizations, chia seeds have gained renewed global popularity for their exceptional nutritional value. Rich in omega-3 fatty acids, antioxidants, fiber, and essential micronutrients, chia is increasingly incorporated into modern health-oriented diets (Al-Younis et al., 2025; Noblat et al., 2025). Beyond traditional use as seeds, chia is now consumed also as sprouts and microgreens (Motyka et al., 2023; Szopa et al., 2023; Huang et al., 2025), expanding its application within functional foods. Microgreens, in particular, are characterized by a high concentration of bioactive compounds, exhibiting active metabolic profiles and enhanced accumulation of secondary metabolites, including phenolics, vitamins, and antioxidants. Moreover, and can be produced rapidly with minimal resource input and space requirements (Kyriacou et al., 2017; Borrelli et al., 2026). These features make them also particularly attractive candidates for space-based

* Corresponding author.
** Corresponding author.
E-mail addresses: sara.defrancesco@unina.it (S. De Francesco), chiara.amitrano@unina.it (C. Amitrano), ermenegilda.vitale@unina.it (E. Vitale), w.tinganelli@gsi.de (W. Tinganelli), marco.durante@unina.it (M. Durante), depascal@unina.it (S. De Pascale), carmen.arena@unina.it (C. Arena), demicco@unina.it (V. De Micco).

https://doi.org/10.1016/j.plaphy.2026.111517
Received 5 February 2026; Received in revised form 29 May 2026; Accepted 25 June 2026
Available online 26 June 2026

cultivation systems to support astronauts' health (Teng et al., 2023; De Francesco et al., 2023).

However, plants cultivated in space must withstand unique abiotic stresses, including ionizing radiation, a major factor in space environments that can impair growth, alter metabolism, and damage cellular structures. Space radiation is a complex and unique radiation environment that poses significant risks to both astronauts and biological systems. It consists of protons and helium nuclei essentially, and only for 1% of heavy ions, like carbon and iron. Although present in relatively low abundance within Galactic Cosmic Rays (GCRs), these ions have a disproportionately strong biological impact due to their high linear energy transfer. At the cellular level, ionizing radiation induces the production of reactive oxygen species (ROS), leading to oxidative stress and perturbations in photosynthesis and primary metabolism. These changes can activate antioxidant defenses and metabolic adjustments, affecting the accumulation of bioactive compounds and, consequently, the nutritional quality of plant tissues (De Micco et al., 2022). Understanding plant responses to such radiation is therefore essential for evaluating their suitability for space farming. Previous studies have primarily focused on model species or leafy greens (De Micco et al., 2023a, 2023b; Amitrano et al., 2024; De Francesco et al., 2025), highlighting a gap in the investigation of alternative species as emerging crops increasingly integrated into modern diets.

Although chia seeds have been extensively studied for their health-promoting properties and potential therapeutic value (De Falco et al., 2017; Biswas et al., 2023), chia sprouts and microgreens are emerging as nutraceutical plant materials (Motyka et al., 2023; Szopa et al., 2023) and may also be suitable for space-related applications; however, to the best of our knowledge, they have not yet been investigated in this context.

This study aimed to evaluate the response of chia microgreens to ionizing radiation, exposing dry seeds to increasing doses of carbon and iron heavy ions (0.3, 1, 10, 20, and 25 Gy), two representative components of galactic cosmic rays. By examining morphological, anatomical, and biochemical responses to different doses of such heavy ions, this research aims to provide insights into potential ion-specific acclimation responses and the potential role of this species for space farming. By assessing multiple traits and their variation under radiation stress, this study seeks to explore the phenotypic plasticity of chia microgreens as a key determinant of their acclimation potential in extreme environments.

2. Materials and methods

2.1. Plant material and irradiation treatments

Salvia hispanica L. seeds were sourced from a local supplier (Fertitecnica Colfiorito SRL located in Colfiorito, Italy) and irradiated with heavy ions at the SIS18 of the GSI Helmholtzzentrum für Schwerionenforschung in Darmstadt, Germany. Samples were exposed to carbon ions (C-ions, ^{12}C isotope, 240 MeV/n) or iron-ions (Fe-ions, ^{56}Fe isotope, 1 GeV/n) at the doses of 0.3, 1, 10, 20, and 25 Gy. Details of dosimetry in the GSI vault are reported in Luoni et al. (2020). For comparison, the Linear energy Transfer (LET) in water is about 15 keV/μm for C-ions and 147 keV/μm for Fe-ions. Non-irradiated control seeds were transported and handled under the same environmental and logistical conditions as the irradiated samples, to ensure that any observed effects were attributable solely to radiation exposure.

2.2. Plant cultivation

After the irradiation treatment, dry seeds were divided into four replicates per dose (250 seeds per replicate), sown in pots (diameter: 7.5 cm; height: 4 cm) filled with standard horticultural soil, and placed in a growth chamber under controlled environmental conditions (temperature: 24 ± 2 °C; relative humidity: 70 ± 10%). To promote uniform germination, seeds were initially maintained in darkness conditions. Upon visible radicle emergence, pots were transferred to a photoperiodic regime consisting of white LED illumination (200 ± 20 μmol photons m^{-2} s^{-1} photosynthetic photon flux density, PPFD) with a 12 h light/12 h dark cycle (lights on from 08:00 to 20:00). Nine days after sowing (DAS), microgreens were subjected to eco-physiological analyses, while, at 10 DAS, they were harvested by cutting them at the base to perform morpho-biometric, anatomical, and biochemical analyses.

2.3. Eco-physiological analyses and sampling

Leaf gas exchange measurements were carried out on all pots per dose and control treatments. Net CO_2 assimilation rate (P_N), stomatal conductance (g_s), and transpiration (E) were measured using an airflow rate within the range of 200–300 μmol s^{-1} at ambient CO_2 concentration (430 μmol mol^{-1}) and ambient temperature (25 °C), with a portable infrared gas-analyzer (LCA 4; ADC, BioScientific, Hoddesdon, UK) equipped with a versatile chamber (surface area of 45.34 cm^2), allowing gas exchange measurements on the entire above-ground canopy within a single pot as reported in Amitrano et al. (2025).

Microgreens were then sampled for biometric, microscopy, and biochemical analyses (10 microgreens per pot per each type of analysis). Fresh and dry biomass of the whole canopy were calculated per unit growing area and expressed as kg m^{-2} and g m^{-2}, respectively (Amitrano et al., 2023). The dry weight was obtained after drying the samples in an oven at 60 °C until they reached a constant weight.

2.4. Biometric and anatomical analyses

Hypocotyl length was measured on digital images, analyzed using ImageJ software (U.S. National Institutes of Health, Bethesda, MD, USA).

Microgreens collected for microscopy analyses were fixed in the F.A.A. chemical fixative (5 mL of 40% formaldehyde, 5 mL of glacial acetic acid, 90 mL of 50% ethanol). Sub-samples of cotyledons (5 × 6 mm, $n = 3$ per dose) were dissected and subjected to dehydration (through ethanol series up to 100%), infiltration, and inclusion in an acrylic resin (JB4®, Polysciences, Eppelheim, Germany). These sub-samples were sectioned with a rotary microtome (PFM rotary 3004 M, PFM Medical, Cologne, Germany) obtaining cross sections (5 μm thick). Half of the sections were stained with Toluidine Blue O at 0.5% in distilled water (Feder and O'Brien, 1968), mounted with mineral oil, and observed under a transmitted light microscope (BX 53, Olympus, Hamburg, Germany). Digital images were acquired with a camera (Olympus EP50), and the software CellSens 2.3 (Olympus, Tokyo, Japan) was used to analyze and quantify functional anatomical parameters. Specifically, in each section, the total thickness of the leaf lamina, upper epidermis thickness, lower epidermis thickness, palisade parenchyma thickness, and spongy parenchyma thickness were measured at three points of the section. Furthermore, the percentage of intercellular spaces in the spongy parenchyma was also measured in three regions of the section. The other half of the cross sections, not stained, were observed under an epi-fluorescence microscope (BX 53, Olympus) equipped with a mercury lamp, band-pass filter of 330–385 nm, dichromatic mirror of 400 nm and above, and a barrier filter of 420 nm and above (Fukuzawa and Fujii, 1992; Ruzin, 2024), to visualize UV-induced autofluorescence associated with phenolic-related compounds in the mesophyll. UV-induced autofluorescence was used as a qualitative indicator of the relative abundance and spatial distribution of phenolic-related autofluorescent compounds in palisade and spongy parenchyma tissues. Fluorescence intensity was measured as the mean gray value in three areas for both palisade and spongy parenchyma according to De Micco et al. (2014; 2020).

Table 1
Effects of ion type, dose, and their interaction on fresh biomass, dry biomass, microgreens length, transpiration rate (E), stomatal conductance (gs) and net photosynthesis (P_N) of *S. hispanica* L. microgreens from the control (0) and irradiated seeds with increasing doses (0.3, 1, 10, 20, 25 Gy) of C- and Fe-ions. Mean values and standard errors are shown. Different letters correspond to significant differences among irradiation doses according to the Student–Newman–Keuls multiple comparison tests ($p \leq 0.05$). NS: not significant; *, **, ***: significant at $p < 0.05$, 0.01, and 0.001, respectively.

	Fresh Biomass (Kg/m^2)	Dry Biomass (g/m^2)	Microgreens lenght (cm)	E (mol H_2O m^{-2} s^{-1})	gs (mmol H_2O m^{-2} s^{-1})	P_N (mmol CO_2 m^{-2} s^{-1})
Ion						
^{12}C	1.87 ± 0.03 a	157 ± 2.49 b	4.06 ± 0.04 b	1.02 ± 0.06 a	0.08 ± 0.006 a	3.00 ± 0.19 a
^{56}Fe	1.92 ± 0.03 a	168 ± 3.91 a	4.37 ± 0.05 a	0.75 ± 0.03 b	0.06 ± 0.002 b	3.41 ± 0.20 a
Dose (Gy)						
0	1.80 ± 0.04 b	152 ± 4.35 a	4.04 ± 0.06 bc	0.76 ± 0.07 a	0.06 ± 0.01 a	3.22 ± 0.33 a
0.3	1.93 ± 0.04 a	170 ± 5.27 a	4.23 ± 0.1 ab	0.88 ± 0.13 a	0.07 ± 0.01 a	3.31 ± 0.11 a
1	1.93 ± 0.05 a	167 ± 5.56 a	3.85 ± 0.05 c	0.98 ± 0.10 a	0.08 ± 0.02 a	2.52 ± 0.17 a
10	2.02 ± 0.03 a	168 ± 3.51 a	4.49 ± 0.09 a	0.95 ± 0.11 a	0.08 ± 0.01 a	3.43 ± 0.35 a
20	1.91 ± 0.03 ab	162 ± 5.64 a	4.32 ± 0.06 a	0.89 ± 0.09 a	0.06 ± 0.01 a	3.65 ± 0.33 a
25	1.79 ± 0.06 b	155 ± 8.91 a	4.36 ± 0.07 a	0.82 ± 0.10 a	0.06 ± 0.01 a	3.01 ± 0.55 a
Significance						
Ion	NS	*	***	***	**	NS
Dose	**	NS	***	NS	NS	NS
Ion x Dose	NS	NS	***	NS	NS	NS

2.5. Biochemical analyses

2.5.1. Minerals and organic acid content

Mineral content analyses were conducted on dried samples (3 replicates of 0.250 g per dose), which were processed using a model MF10.1 grinding mill (IKA-Werke GmbH & Co. KG, Staufen, Germany). Minerals (Ammonium, Nitrite, Nitrate, Sulfate, Phosphate, Sodium, Potassium, Magnesium, Calcium, Chloride) and organic acid (Oxalate, Tartrate, Malate, Citrate, Isocitrate) composition was determined using ICS-3000 ion chromatography equipment (Dionex, Sunnyvale, CA, USA). Anionic and cationic separations were obtained via the IonPac AS11-HC and IonPac CS12A analytical columns and quantified against chromatography standards using electrical conductivity detectors (Dionex, Sunnyvale, CA, USA) as mentioned in detail by Rouphael et al. (2017). All mineral and organic acids contents are quantified as mg 100 g^{-1} DW.

2.5.2. Antioxidant, pigment and protein determination

For the biochemical analyses, microgreens collected at the harvest were immediately frozen at −20 °C. The antioxidant capacity was determined by Ferric Reducing Antioxidant Power (FRAP) assay following the procedure reported in Vitale et al. (2020, 2021a). Briefly, for each dose, four replicates (0.250 g each) were ground in liquid nitrogen treated with a 60:40 methanol/water solution and centrifuged at 14,000 rpm for 15 min at 4 °C. The FRAP reagents (300 mM acetate buffer pH 3.6, 1:16.6 *v/v*; 10 mM tripyridyl triazine, TPTZ, in 40 mM HCl, 1:11.6 *v/v*; 12 mM FeCl3, 1:11.6 *v/v*) were combined with the extracts and incubated for 1 h in the dark. Then, the absorbance was read at 593 nm by a spectrophotometer (UV-VIS Cary 100; Agilent Technologies, Palo Alto, CA, USA). The antioxidant capacity was calculated using a Trolox standard curve and expressed as micromole of Trolox equivalents per gram of fresh weight (μmol Trolox eq g^{-1} FW).

For the total content of chlorophylls ($a + b$) and carotenoids ($x + c$) determination, powdered samples (four replicates of 0.2 g per each dose) (Vitale et al., 2021b) were homogenized in ice-cold 100% acetone using a mortar and pestle. The extracts were centrifuged at 5000 rpm for 5 min in a Labofuge GL (Heraeus Sepatech, Hanau, Germany). Afterward, the absorbance of supernatants was determined using a UV-VIS Cary 100 spectrophotometer from Agilent Technologies at wavelengths of 470, 645, and 662 nm. Pigment concentration was quantified following the equations reported in Lichtenthaler (1987).

Total polyphenols were determined as reported in Arena et al., (2019). Briefly, Powdered samples (four replicates of 0.2 g per each dose) were extracted in methanol at 4 °C and centrifuged at 11,000 rpm for 5 min. The soluble fraction was mixed with 10% Folin–Ciocalteu solution in a ratio of 1:1 *v/v* for 3 min and then treated with 700 mM Na_2CO_3 solution in a ratio of 1:5, *v/v*. Samples were incubated for 2 h in the darkness. The absorbance was measured at 765 nm with a spectrophotometer (UV-VIS Cary 100; Agilent Technologies) and the content of total polyphenol was expressed as milligrams of gallic acid equivalents per gram of fresh weight (mg GAE g^{-1} FW) using a gallic acid standard curve.

Total soluble protein content was determined according to Bradford (1976) and Im et al., (2017). Powdered samples (four replicates of 0.2 g per each dose) were homogenized in 0.2 M potassium phosphate buffer and then centrifuged at 10,000 rpm at 4 °C. The supernatant absorbance was read at 595 nm by a spectrophotometer (UV-VIS Cary 100, Agilent Technologies, Palo Alto, CA, USA). The protein concentration was expressed as micrograms of BSA (bovine serum albumin) equivalents (μg BSA eq. g^{-1} FW) per gram of fresh weight using the BSA to build a standard curve.

Antioxidant capacity, pigments, polyphenols and soluble proteins were expressed on a fresh weight basis to reflect their physiological relevance in the edible product, whereas mineral contents were expressed on a dry weight basis to allow accurate comparisons independent of tissue water content.

2.6. Trait-level phenotypic plasticity analysis

To assess the responsiveness of morphological and functional traits to ionizing radiation, we calculated the Phenotypic Plasticity Index (PPI) for a total of 11 traits (6 anatomical and 5 biochemical), across increasing doses of C- and Fe-ion irradiation. The PPI was computed for each trait and radiation type according to the following formula:

PPI(trait) = (Maximum trait value across doses − Minimum trait value across doses) / Maximum trait value across doses

This index provides a unitless measure of the relative phenotypic variation observed across treatments, ranging from 0 (no plasticity) to 1 (maximum plasticity), and has been previously used in ecological studies (Valladares et al., 2006). Anatomical traits included total leaf lamina thickness, palisade and spongy parenchyma thickness, intercellular spaces, and fluorescence intensity in palisade and spongy tissues. Biochemical traits included total chlorophylls, carotenoids, antioxidant capacity, total polyphenols, and soluble protein content. PPI values were visualized using a grouped bar plot, where each trait was represented by 2 bars (C-ions and Fe-ions), and then compared across trait types to evaluate the overall trends in plasticity. A heatmap of PPI values and the

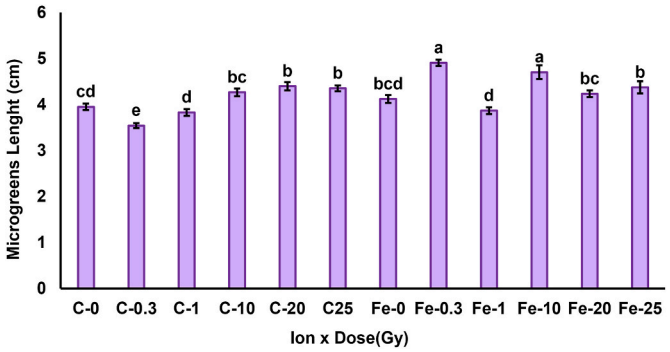

Fig. 1. Effects of the interaction Ion x Dose in *S. hispanica* L. microgreens length. Mean values and standard errors are shown. Different letters correspond to significant differences among irradiation doses according to the Student–Newman–Keuls multiple comparison tests ($p \leq 0.05$).

full dataset were included in the supplementary materials to support data interpretation.

2.7. Statistical analyses

Data were analyzed through two-way analysis of variance (ANOVA) considering the type of ion and the dose delivered as main factors and their interaction (Ion x Dose), using SPSS statistical package (SPSS Inc., Chicago, IL, USA) and the SNK (Student–Newman–Keuls) multiple comparison tests ($p \leq 0.05$). To check for normality, the Kolmogorov–Smirnov test was applied; the arcsine transformation function was applied to percentage of intercellular spaces before statistical analysis. Principal Component Analysis (PCA) was performed to explore the relationships among morphological, physiological, and biochemical traits measured across all treatments. Prior to analysis, all variables were checked for normality and autoscaled (mean-centered and divided by their standard deviation) to ensure equal weighting of parameters with different units. PCA was conducted in R (v4.4.0) using the *prcomp* () function with *center* = TRUE and *scale.* = TRUE. Biplots were generated using *ggplot2* and *ggrepel* R packages to display both sample scores and variable loadings without label overlap. Variables contributing most to each principal component were identified from the loadings matrix and interpreted in the context of plant functional responses to irradiation

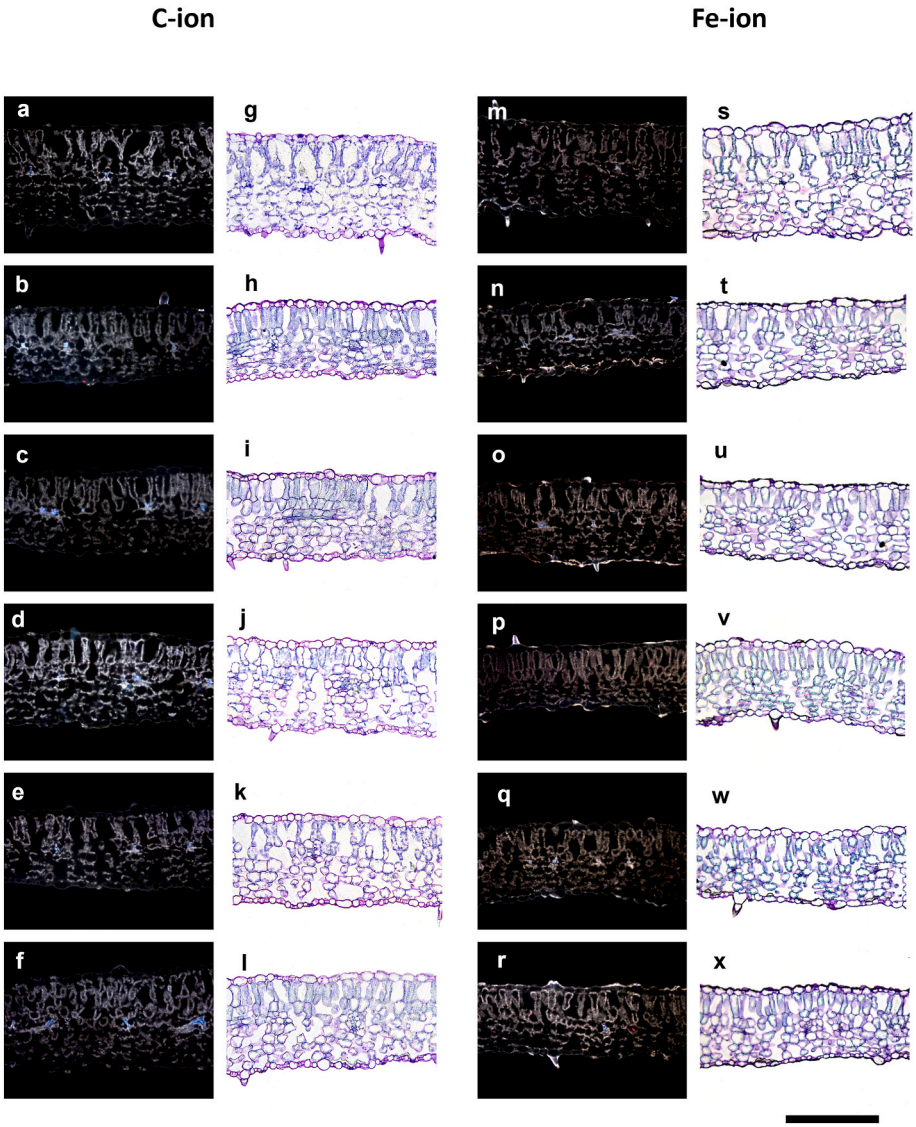

Fig. 2. Epi-fluorescence (a–f, m–r) and light (g–l, s–x) microscopy images of cross sections of *S. hispanica* L. cotyledons from control seeds (0 Gy; a, g, m, s) and seeds irradiated with increasing doses of C-ions (0.3 Gy: b, h; 1 Gy: c, i; 10 Gy: d, j; 20 Gy: e, k; 25 Gy: f, l) and Fe-ions (0.3 Gy: n, t; 1 Gy: o, u; 10 Gy: p, v; 20 Gy: q, w; 25 Gy: r, x). Epi-fluorescence images show UV-induced autofluorescence associated with phenolic-related compounds in mesophyll tissues. All images were acquired at the same magnification. Scale bar = 200 μm.

Table 2
Effects of ion type, dose, and their interaction on the thickness of Total leaf lamina, Upper Epidermis, Palisade Parenchyma, Spongy Parenchyma, Lower Epidermis, percent of Intercellular spaces, Fluorescence intensity of Palisade and Spongy parenchyma tissues of cotyledons of *S. hispanica* L. microgreens from the control (0) and irradiated seeds with increasing doses (0.3, 1, 10, 20, 25 Gy) of C- and Fe-ions. Mean values and standard errors are shown. Different letters correspond to significant differences among irradiation doses according to the Student–Newman–Keuls multiple comparison tests ($p \leq 0.05$). NS: not significant; *, **, ***: significant at $p < 0.05$, 0.01, and 0.001, respectively.

	Total leaf lamina	Upper Epidermis	Palisade Parenchyma	Spongy Parenchyma	Lower Epidermis	Intercellular spaces (spongy parenchyma)	Palisade Fluorescence Intensity	Spongy Fluorescence Intensity
	(μm)	(μm)	(μm)	(μm)	(μm)	(%)		
Ion								
^{12}C	269 ± 2.63 a	22.1 ± 0.439 a	101 ± 0.969 a	128 ± 2.17 a	16.5 ± 0.349 b	36.6 ± 1.13 a	32.1 ± 0.839 b	19.0 ± 0.540 b
^{56}Fe	229 ± 3.41 b	22.8 ± 0.454 a	89.0 ± 1.25 b	102 ± 2.44 b	17.6 ± 0.379 a	32.3 ± 0.901 b	37.6 ± 0.903 a	26.9 ± 0.852 a
Dose (Gy)								
0	272 ± 4.42 a	23.1 ± 0.964 a	105 ± 1.67 a	126 ± 3.64 a	18.5 ± 0.662 a	36.9 ± 1.92 a	31.3 ± 1.08 b	20.6 ± 0.846 b
0.3	232 ± 6.14 b	22.6 ± 0.816 a	86.0 ± 2.28 c	107 ± 4.55 b	16.8 ± 0.640 ab	34.5 ± 1.97 ab	30.1 ± 1.39 b	21.5 ± 0.71 b
1	246 ± 5.56 b	22.5 ± 0.759 a	93.3 ± 1.83 b	116 ± 4.16 ab	15.0 ± 0.581 b	32.6 ± 1.55 ab	38.4 ± 1.20 a	22.7 ± 1.17 b
10	253 ± 5.74 b	22.6 ± 0.780 a	93.5 ± 1.91 b	120 ± 4.11 ab	17.7 ± 0.611 a	38.0 ± 1.85 a	33.3 ± 1.52 b	21.6 ± 1.25 b
20	249 ± 3.55b	22.6 ± 0.658 a	97.5 ± 1.36 b	112 ± 3.22 ab	17.7 ± 0.703 a	35.0 ± 1.83 ab	33.5 ± 1.73 b	23.5 ± 1.94 b
25	242 ± 7.96 b	21.3 ± 0.633 a	94.1 ± 2.52 b	110 ± 5.80 ab	16.4 ± 0.502 ab	29.9 ± 1.40 b	42.3 ± 1.53 a	27.7 ± 1.78 a
Significance								
Ion	***	NS	***	***	*	**	***	***
Dose	***	NS	***	**	**	*	***	***
Ion x Dose	***	NS	***	***	NS	**	***	***

treatments.

3. Results

3.1. Morpho-anatomical and eco-physiological analyses

Microgreens growth was not prevented in any of the treatments, and no visible signs of damage were observed. In Table 1, the main effects of the ion type, dose, and their interaction on fresh and dry biomass, microgreens length, transpiration rate, stomatal conductance, and net photosynthesis are reported. The ion type significantly affected dry biomass, microgreens length, transpiration rate, and stomatal conductance. Specifically, Fe-ion irradiation increased dry biomass and microgreens length, while reducing transpiration rate and stomatal conductance.

The dose alone significantly influenced only fresh biomass and microgreens length. Compared to the control and 25 Gy, doses of 0.3, 1, and 10 Gy, significantly increased fresh biomass, while microgreens length increased significantly at doses ≥10 Gy compared to the control. A significant interaction effect was found for length (Fig. 1), with Fe-irradiation at 0.3 and 10 Gy (Fe-0.3 and Fe-10) inducing significantly higher values than the controls and other doses.

3.2. Anatomical analyses

Exposure to increasing doses of carbon and iron ions did not result in visible alterations in tissue organization or delays in tissue differentiation (Fig. 2). However, quantitative analysis showed significant changes in anatomical traits.

Ion type significantly affected all anatomical parameters analyzed except for the upper epidermis thickness (Table 2). Specifically, cotyledons derived from C-ion–irradiated seeds exhibited greater leaf lamina thickness, associated with thicker palisade and spongy parenchyma and increased intercellular spaces, compared to those from Fe-ion–irradiated seeds. Fe-ion exposure increased the lower epidermis thickness and fluorescence intensity in both parenchyma tissues compared to C-ions treatment.

Similarly, the dose effect was significant for all anatomical parameters measured, excluding the upper epidermis thickness. Compared to the control, all irradiation doses reduced the total leaf lamina thickness, mainly due to significantly thinner palisade parenchyma, which reached the minimum value at 0.3 Gy. Spongy parenchyma was significantly thinner in cotyledons from seeds irradiated at 0.3 Gy than the control, while lower epidermis was significantly reduced by the 1Gy treatment compared to the control. The percentage of intercellular spaces was significantly reduced only by 25 Gy compared to the control and 10 Gy. Fluorescence intensity increased at 1 and 25 Gy within the palisade parenchyma, while only at 25 Gy within the spongy parenchyma, compared to the control and the other doses.

The interaction between the factors was significant for all analyzed parameters except for the thickness of both epidermic tissues (Table 2). Specifically, for total leaf lamina (Fig. 3a) and spongy parenchyma thickness (3c), C-ions at 10 and 25 Gy (C-10 and C-25) determined the occurrence of higher values compared to the control and the other treatments, whereas Fe-ions at 0.3, 10, 20 and 25 Gy (Fe-0.3, Fe-10, Fe-20, and Fe-25) determined significantly lower values than controls. For palisade parenchyma thickness (3b), similar trends were observed, with Fe-0.3, Fe-10, and Fe-25 showing significantly lower values than the control and other doses. In terms of intercellular spaces (Fig. 3d), C-10 showed the highest value which was significantly higher than C-0.3, C-25 and Fe-treatments starting from 1 Gy. Lastly, regarding the UV-induced autofluorescence intensity in palisade (Fig. 3e) and spongy parenchyma (Fig. 3f), treatments Fe-1, Fe-20, and Fe-25 showed significantly higher values than most of the other treatments.

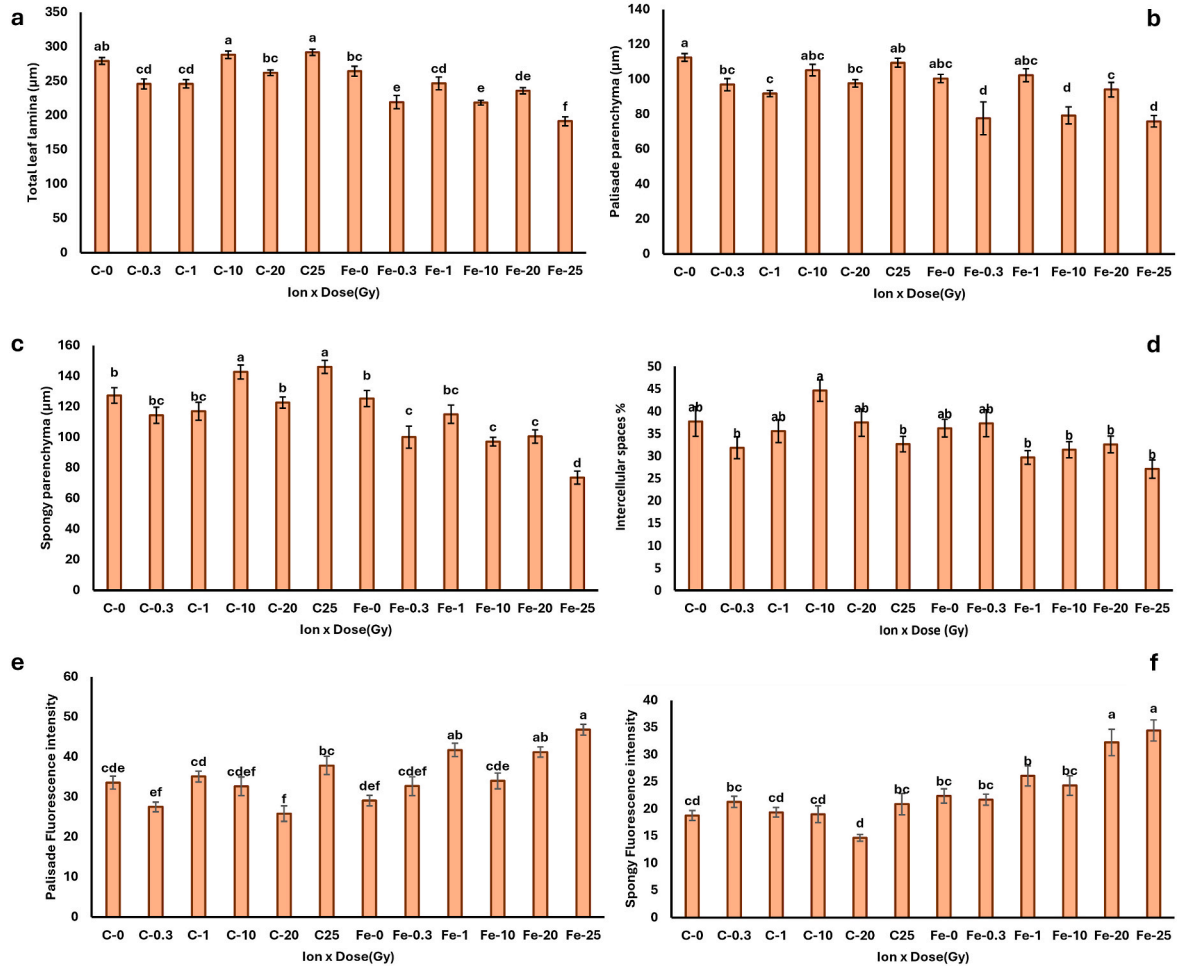

Fig. 3. Effects of the interaction between ion type and dose (Ion × Dose) on total leaf lamina thickness (a), palisade (b) and spongy (c) parenchyma thickness, percentage of intercellular spaces (d), and UV-induced autofluorescence intensity in palisade (e) and spongy (f) parenchyma of *S. hispanica* L. microgreen cotyledons derived from seeds irradiated with C- and Fe-ions. Values represent means ± SE. Different letters indicate significant differences among treatments according to the Student–Newman–Keuls test ($p \leq 0.05$).

3.3. Biochemical analysis

Mineral composition, (Table 3), revealed that all elements, except sodium, were influenced by the ion type. Carbon ion irradiation enhanced nitrite, nitrate, sulfate, phosphate, potassium, magnesium, calcium, and chloride, whereas iron irradiation increased ammonium content. Dose as main factor was significant solely for calcium, where the high doses of 20 and 25 Gy resulted in a significant rise relative to both the control and the other doses.

Lastly, the interaction (Table 3, Fig. S1.) between the main factors influenced only sodium and calcium. In the case of sodium, significant increases were observed under the Fe-25 treatment compared to all the other treatments except for Fe-0.3, Fe-20, C-0.3 and C-1. Calcium content showed a dose-dependent increase under C-ion irradiation, whereas no clear trend was observed under Fe-ion treatments.

The different treatments also had a significant impact on the concentration of organic acids (Table 4). Specifically, the ion type significantly influenced oxalate, malate, and isocitrate: C-ion irradiation increased oxalate and malate contents, while Fe-ion treatments increased isocitrate. The dose effect was significant only for oxalate and citrate content. Compared to the control, the high dose of 25 Gy led to increased citrate levels relative to the other doses. Oxalate content showed significantly higher values at 20 Gy compared to the control and C-0.3 treatment. The interaction between the main factors did not significantly influence the analyzed parameters.

Regarding antioxidant capacity, chlorophylls, carotenoids, soluble proteins, and total polyphenols (Table 5), the ion had a significant effect only on chlorophylls, carotenoids, and polyphenols. In particular, exposure to Fe-ions resulted in a significant increase in chlorophyll and carotenoid concentrations, accompanied by a decrease in total polyphenols compared to the C-ion treatment.

Radiation dose significantly influenced all parameters, generally showing an increase with rising doses, followed by a decrease, although the dose at which maximum value occurred varied depending on the parameter analyzed. Interestingly, the antioxidant capacity showed significantly higher values at 0.3 Gy compared with the control and all other treatments. Chlorophyll and carotenoid contents were significantly higher at 10 Gy compared with the control and all other doses. Low doses (0.3–1 Gy) increased soluble protein content, whereas high doses (20–25 Gy) resulted in a decrease relative to the control. Lastly, total polyphenols showed significantly higher values at 1 Gy compared with 25 Gy.

The interaction between factors (Table 5, Fig. 4) was significant for all biochemical parameters. Specifically, Fe-ion exerted stronger effects at low doses, enhancing antioxidant capacity (4a) at 0.3 Gy and proteins (4c) at 0.3, 1, and 10 Gy. In contrast, C-ion treatment more effectively increased total polyphenol content (4a) at 0.3–1 Gy. Both ions showed similar trends for pigment levels (4b), with an increase at intermediate doses followed by a decline at higher doses.

Table 3
Effects of ion type, dose, and their interaction on mineral composition of *S. hispanica* L. microgreens from the control (0) and seedlings irradiated with increasing doses (0.3, 1, 10, 20, 25 Gy) of C- and Fe-ions. Mean values and standard errors are shown. Different letters correspond to significant differences among irradiation doses according to the Student–Newman–Keuls multiple comparison tests ($p \leq 0.05$). NS: not significant; *, **, ***: significant at $p < 0.05$, 0.01, and 0.001, respectively.

	Ammonium	Nitrite	Nitrate	Sulfate	Phosphate	Sodium	Potassium	Magnesium	Calcium	Chloride
	(g/kg d.m.)									
Ion										
^{12}C	0.410 ± 0.011 b	0.044 ± 0.002 a	0.420 ± 0.018 a	20.7 ± 0.42 a	9.23 ± 0.12 a	0.162 ± 0.007 a	21.9 ± 0.41 a	5.07 ± 0.07 a	5.65 ± 0.13 a	7.92 ± 0.15 a
^{56}Fe	0.580 ± 0.041 a	0.033 ± 0.002 b	0.126 ± 0.036 b	15.1 ± 0.73 b	8.76 ± 0.17 b	0.179 ± 0.016 a	20.4 ± 0.35 b	4.71 ± 0.11 b	5.19 ± 0.11 b	7.14 ± 0.14 b
Dose (Gy)										
0	0.463 ± 0.046 a	0.037 ± 0.005 a	0.338 ± 0.073 a	18.3 ± 1.21 a	8.87 ± 0.21 a	0.163 ± 0.011 a	21.4 ± 0.80 a	4.87 ± 0.14 a	5.08 ± 0.12 b	7.37 ± 0.43 a
0.3	0.424 ± 0.028 a	0.039 ± 0.006 a	0.332 ± 0.048 a	17.2 ± 1.25 a	8.58 ± 0.3 a	0.186 ± 0.016 a	20.6 ± 0.59 a	4.64 ± 0.17 a	5.14 ± 0.11 b	7.30 ± 0.24 a
1	0.453 ± 0.047 a	0.037 ± 0.002 a	0.320 ± 0.073 a	17.5 ± 2.14 a	8.87 ± 0.24 a	0.158 ± 0.015 a	21.8 ± 0.54 a	4.85 ± 0.08 a	5.18 ± 0.13 b	7.60 ± 0.17 a
10	0.501 ± 0.082 a	0.043 ± 0.003 a	0.212 ± 0.092 a	17.9 ± 1.31 a	8.82 ± 0.14 a	0.155 ± 0.011 a	20.8 ± 0.69 a	4.90 ± 0.21 a	5.24 ± 0.24 b	7.51 ± 0.29 a
20	0.582 ± 0.091 a	0.035 ± 0.003 a	0.217 ± 0.091 a	19.0 ± 1.73 a	9.38 ± 0.28 a	0.164 ± 0.013 a	21.1 ± 0.83 a	5.07 ± 0.16 a	5.76 ± 0.12 a	7.60 ± 0.29 a
25	0.546 ± 0.056 a	0.043 ± 0.005 a	0.220 ± 0.096 a	17.5 ± 1.99 a	9.41 ± 0.30 a	0.196 ± 0.046 a	21.3 ± 1.00 a	5.02 ± 0.24 a	6.12 ± 0.24 a	7.80 ± 0.35 a
Significance										
Ion	***	**	***	***	*	NS	*	**	***	**
Dose	NS	NS	NS	NS	NS	NS	NS	NS	***	NS
Ion x Dose	NS	NS	NS	NS	NS	*	NS	NS	*	NS

3.4. Principal component analysis

The PCAs (Fig. 5) revealed a clear separation between samples from seeds exposed to C- and Fe-ions, indicating distinct biochemical and physiological responses depending on the radiation type and dose.

In Fig. 5a, the first two principal components explained 54.8% of the total variance (PC1 = 35.1%, PC2 = 19.7%). Along PC1, Fe-irradiated samples were clearly separated from the C-ion treatments, positioned on the opposite sides of the plot.

Variables most strongly correlated with PC1 included DW, chlorophyll, carotenoids, and P_N, characterizing Fe-irradiated plants, in contrast to tissue thickness, transpiration (E), and several organic acids (e.g., tartrate, malate, citrate), which were associated with the C-ion samples.

Along PC2, samples were further differentiated by dose: lower doses (Fe 0.3–1 Gy) clustered in the upper-left quadrant, positively associated with DW and gs, while higher doses (Fe 10–25 Gy) appeared in the lower-left region, linked to a decline in photosynthetic activity (P_N) and to fluorescence parameters (Pfluo, Sfluo). In the case of C-ions, lower doses (C 0.3–1 Gy) clustered in the upper-right quadrant, positively associated with antioxidant capacity, proteins and polyphenols, while higher doses (C 10–25 Gy) appeared in the lower-right region, associated mostly with tissue thickness and organic acids.

The PCA in Fig. 5b was carried out excluding mineral content variables, in order to assess whether the segregation among treatments was primarily driven by mineral profiles or by non-mineral physiological and biochemical traits. In this PCA, PC1 and PC2 explained 32.3% and 24.9% of the total variance, respectively.

PC1 separated Fe-from C-irradiated samples, highlighting that C-ion exposure was mainly associated with metabolic and structural adjustments, while Fe-ion exposure affected photosynthetic and pigment-related parameters. Along PC2, samples showed a dose-dependent distribution, with lower doses mainly associated to antioxidant and polyphenols as well as to water-related parameters (e.g. fresh weight, gs, and E), while higher doses were mainly related to general structural (length and tissue thickness) as well as photosynthetic level.

3.5. Phenotypic Plasticity Index (PPI) analysis

PPI analysis revealed a clear distinction between the plastic responses of biochemical and anatomical traits to ionizing radiation. As shown in Table S1, Fig. 6 and S2, biochemical traits generally exhibited higher PPI values. The most plastic trait was soluble protein content under Fe-ion treatment (PPI = 0.85), followed by polyphenols under C-ion exposure (PPI = 0.71). Antioxidant capacity and pigment-related traits (chlorophyll and carotenoids) also showed moderate plasticity under both radiation types.

In contrast, anatomical traits displayed lower overall plasticity. Palisade thickness and intercellular spaces were the least responsive, with PPI values below 0.3 regardless of radiation type. A modest increase in plasticity was observed for spongy parenchyma thickness under Fe-ion exposure (PPI = 0.41), indicating a potential structural adjustment in response to radiation-induced stress.

These patterns underscore the trait-specific and radiation-type-dependent nature of phenotypic plasticity in chia microgreens.

4. Discussion

This study was based on the hypothesis that different types of high-LET radiation (carbon vs iron ions) would differentially affect morpho-physiological, anatomical, and biochemical traits in chia microgreens. The results largely support this hypothesis, revealing ion- and dose-dependent responses that shape plant development and secondary metabolism, reflecting the phenotypic plasticity of *S. hispanica* under radiation.

From a morpho-physiological perspective, the two ions exhibited

Table 4
Effects of ion type, dose, and their interaction on the content of organic acids in *S. hispanica* L. microgreens from the control (0) and seedlings irradiated with increasing doses (0.3, 1, 10, 20, 25 Gy) of C- and Fe-ions. Mean values and standard errors are shown. Different letters correspond to significant differences among irradiation doses according to the Student–Newman–Keuls multiple comparison tests ($p \leq 0.05$). NS: not significant; *, **, ***: significant at $p < 0.05$, 0.01, and 0.001, respectively.

	Oxalate	Tartrate	Malate	Citrate	Isocitrate
	(g/kg d.m.)				
Ion					
^{12}C	6.15 ± 0.16 a	2.36 ± 0.04 a	11.5 ± 0.24 a	1.29 ± 0.06 a	0.093 ± 0.012 b
^{56}Fe	5.65 ± 0.12 b	2.32 ± 0.03 a	10.6 ± 0.19 b	1.29 ± 0.07 a	0.140 ± 0.019 a
Dose (Gy)					
0	5.48 ± 0.21 b	2.36 ± 0.11 a	11.0 ± 0.36 a	1.10 ± 0.07 c	0.112 ± 0.026 a
0.3	5.45 ± 0.21 b	2.36 ± 0.05 a	10.5 ± 0.35 a	1.08 ± 0.05 c	0.061 ± 0.018 a
1	5.98 ± 0.18 ab	2.36 ± 0.07 a	11.1 ± 0.37 a	1.15 ± 0.04 c	0.103 ± 0.030 a
10	6.06 ± 0.18 ab	2.33 ± 0.04 a	11.0 ± 0.46 a	1.24 ± 0.05 bc	0.123 ± 0.028 a
20	6.37 ± 0.26 a	2.28 ± 0.05 a	11.5 ± 0.41 a	1.41 ± 0.06 b	0.129 ± 0.034 a
25	6.05 ± 0.34 ab	2.36 ± 0.05 a	11.1 ± 0.58 a	1.77 ± 0.08 a	0.172 ± 0.026 a
Significance					
Ion	*	NS	**	NS	*
Dose	*	NS	NS	***	NS
Ion x Dose	NS	NS	NS	NS	NS

Table 5
Effects of ion type, dose, and their interaction on Antioxidant capacity, Chlorophyll (Chl a+b), Carotenoids (Car x + c), Proteins and Polyphenols content in *S. hispanica* L. microgreens from the control (0) and seedlings irradiated with increasing doses (0.3, 1, 10, 20, 25 Gy) of C- and Fe-ions. Mean values and standard errors are shown. Different letters correspond to significant differences among irradiation doses according to the Student–Newman–Keuls multiple comparison tests ($p \leq 0.05$). NS: not significant; *, **, ***: significant at $p < 0.05$, 0.01, and 0.001, respectively.

	Antioxidant Capacity	Chl a+b	Car x + c	Proteins	Poliphenols
	μmol Trolox Equivalent (TE) g^{-1} FW	mg g^{-1}	mg g^{-1}	mg eq BSA g^{-1} FW	mg GAE g^{-1} FW
Ion					
Carbon	1.10 ± 0.03 a	1.35 ± 0.08 b	0.20 ± 0.01 b	0.21 ± 0.01 a	1.70 ± 0.14 a
Iron	1.18 ± 0.08 a	1.69 ± 0.09 a	0.26 ± 0.01 a	0.21 ± 0.03 a	1.27 ± 0.06 b
Dose					
0 (Gy)	1.09 ± 0.07 bc	1.35 ± 0.05 b	0.21 ± 0.01 b	0.21 ± 0.01 b	1.31 ± 0.10 ab
0.3 (Gy)	1.52 ± 0.15 a	1.31 ± 0.16 b	0.20 ± 0.03 b	0.28 ± 0.02 a	1.66 ± 0.31 ab
1 (Gy)	1.27 ± 0.04 b	1.56 ± 0.10 b	0.23 ± 0.02 b	0.29 ± 0.02 a	1.95 ± 0.22 a
10 (Gy)	0.99 ± 0.07 c	1.96 ± 0.18 a	0.29 ± 0.03 a	0.24 ± 0.03 ab	1.55 ± 0.1 ab
20 (Gy)	1.02 ± 0.08 c	1.65 ± 0.12 b	0.24 ± 0.02 ab	0.13 ± 0.03 c	1.44 ± 0.07 ab
25 (Gy)	0.92 ± 0.03 c	1.31 ± 0.14 b	0.19 ± 0.02 b	0.13 ± 0.03 c	1.02 ± 0.13 b
Significance					
Ion	NS	***	***	NS	***
Dose	***	***	**	***	***
Ion x Dose	***	**	**	***	***

distinct effects on dry biomass, microgreens length, transpiration rate, and stomatal conductance. Specifically, Fe-ion irradiation promoted dry biomass accumulation and shoot elongation, whereas C-ion exposure increased stomatal conductance and transpiration, likely suggesting different water use and resource allocation strategies. Although net photosynthesis (P_N) did not differ significantly among treatments when analyzed individually, it contributed to sample separation in the PCA through its covariation with other morpho-physiological and biochemical traits. Indeed, irradiated microgreens at low doses enhanced the production of polyphenols at the expense of chlorophyll and carotenoids, suggesting activation of the phenylpropanoid pathway, which is involved in phenolics biosynthesis (Ferreira and Antunes, 2021). This could reflect a general response to stress, potentially enhancing the plant's ability to cope with oxidative stress and other environmental challenges. This aligns with the increase in antioxidant content reported by Vitale et al. (2022) in *B. vulgaris* exposed to carbon ions at 10 Gy.

In the present study, higher doses (≥10 Gy) generally promote microgreen elongation. Under Fe-ion treatment, maximum elongation was observed at 0.3 and 10 Gy, suggesting that specific doses may stimulate metabolic pathways that promote elongation. Notably, at 10 Gy, iron irradiation also enhanced the accumulation of photosynthetic pigments, indicating a coordinated investment in both structural growth and photosynthetic capacity. This elongation may help microgreens optimize light capture under stress, enhancing competitiveness in suboptimal conditions despite unchanged photosynthetic efficiency (Volkova et al., 2022; Cai and Huq, 2025).

Comparisons with other studies underscore the species-specific nature of responses to heavy ion radiation. In previous investigations on five microgreens species exposed to C- and Fe-ions at equivalent doses (0.3–25 Gy) (Amitrano et al., 2024), basil and rocket exhibited reduced elongation under iron irradiation, favoring secondary metabolite accumulation over structural growth, whereas radish and cress showed increased elongation. Comparable patterns were observed in *B. rapa*, where iron ions promoted leaf lamina expansion and maintained metabolic activity, while carbon ions enhanced fresh biomass and elongation without affecting dry weight (De Francesco et al., 2025).

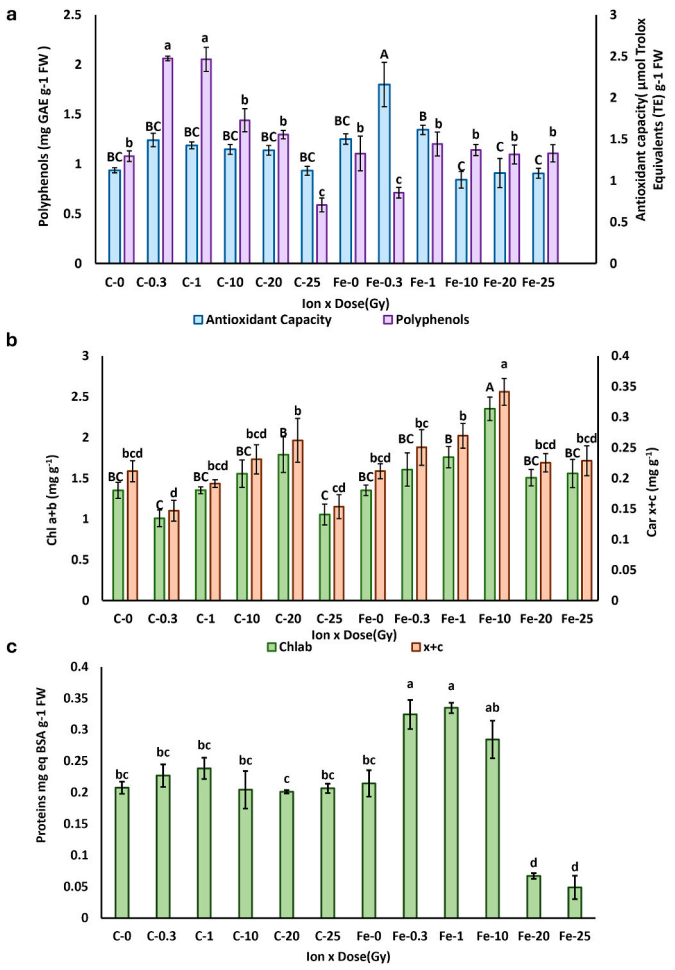

Fig. 4. Effects of interaction (IonxDose) on Polyphenols and Antioxidant capacity (a), Total chlorophyll (chl a+b) and Total carotenoids (x+c) (b) and Protein (c) content in *S. hispanica* L. microgreens. Mean values and standard errors are shown. Different letters correspond to significant differences among irradiation doses according to the Student–Newman–Keuls multiple comparison tests ($p \leq 0.05$).

Anatomical responses were ion-specific too. Although most irradiation doses generally tended to reduce cotyledon lamina thickness compared to the control, in microgreens from C-irradiated seeds this effect was not observed at doses ≥10 Gy, where lamina thickness remained comparable to the control. The observed increase in intercellular spaces, spongy mesophyll, and palisade layer at these doses may facilitate CO_2 diffusion, potentially contributing to physiological compensation under stress. These adaptations could help maintain photosynthetic performance despite structural constraints (Amitrano et al., 2022).

In contrast, Fe-ion treatment resulted in more compact mesophyll tissues with reduced intercellular spaces, particularly at higher doses. This tissue compaction may contribute to the increased UV-induced autofluorescence observed in both palisade and spongy parenchyma under Fe irradiation, consistent with changes in the distribution and relative abundance of phenolic-related autofluorescent compounds at the tissue level.

These observations further support the idea that the two ion types elicit distinct anatomical and physiological strategies: iron ions appear to enhance photosynthetic performance primarily through increased shoot elongation and pigment accumulation, while carbon ions would promote modifications in leaf anatomical structure, potentially favoring stress acclimation through altered mesophyll architecture and enhanced stomatal responsiveness, rather than structural growth. These ion-specific adaptive strategies are further suggested by PCA analysis, which separates the samples based on ion type and highlights the distinct contributions of anatomical versus morpho-physiological traits.

Biochemical data further support ion-specific metabolic adjustments. Carbon ion exposure enhanced essential nutrients (e.g., K, Mg, Ca), potentially driven by increased transpiration allowing plants to improve nutrients' uptake. The increase in the content of these minerals is particularly important for plant health and development, as they play critical roles in various physiological processes, including osmoregulation, enzyme activation, and photosynthetic efficiency (Tariq et al., 2023). In contrast, Fe-ion irradiation enhanced the ammonium levels, likely implying altered nitrogen metabolism (Dubey et al., 2021). Moreover, oxalate accumulation in microgreens from C-ion irradiated seeds, and citrate increases at high doses suggest a shift in organic acid metabolism probably aimed at ROS detoxification (Li et al., 2022; Weir et al., 2006).

Ion type and dose influenced plant biochemical profiles, providing critical insights into stress response dynamics and the activation of secondary metabolism. Carbon and iron irradiation both influenced key metabolic markers, but with distinct trends, suggesting different modes of action and signaling pathways. Under carbon ion exposure, polyphenol levels increased notably at low doses, indicating an early and sustained activation of the phenylpropanoid pathway. A similar low-dose pattern was observed in carbon-ion irradiated lettuce, where polyphenol modulation accompanied enhanced seedling growth and physiological acclimation, supporting the involvement of phenolic-related metabolism in early radiation stress responses (Amitrano et al., 2026).

Notably, both antioxidant capacity and total protein content remained relatively stable and comparable to control levels across all carbon doses, suggesting robust metabolic homeostasis and maintenance of protective mechanisms.

In contrast, iron ion exposure did not elicit a comparable polyphenolic response. Across most doses, polyphenol levels remained similar to those in control plants, whilst at 0.3 Gy, a significant decrease was observed. Interestingly, this dose corresponded to a peak in antioxidant capacity and total protein content, suggesting a distinct, dose-specific adaptation. The inverse relationship between polyphenols and antioxidant capacity at 0.3 Gy implies that, under iron irradiation, antioxidant responses may rely more on non-phenolic compounds or enzymatic ROS-scavenging systems.

The increase in protein content at low to intermediate iron doses may indicate enhanced metabolic activity or structural protein investment, potentially supporting cellular repair and growth. This interpretation is consistent with the observed stimulation of elongation and pigment biosynthesis under iron treatment. Together, these responses suggest a hormetic effect at 0.3 Gy, characterized by beneficial physiological stimulation under mild stress, with potential implications for functional food production in space environments (Douglas et al., 2016).

At higher doses (20–25 Gy), both carbon and iron treatments led to a decline in protein content, with the effect more pronounced under iron irradiation. This suggests a dose-dependent inhibition of protein synthesis or degradation under elevated oxidative stress. Such trends are consistent with responses observed in *Brassica rapa*, where biochemical parameters linked to oxidative metabolism were more sensitive than morphological traits, revealing differential thresholds of damage and species-specific resilience strategies (De Francesco et al., 2025).

The Phenotypic plasticity indices analysis further elucidates the ion- and dose-specific responses observed at the individual trait level. Biochemical traits exhibited higher plasticity than anatomical traits, particularly under iron-ion irradiation, indicating a strong metabolic responsiveness. The high PPI values of soluble protein and antioxidant-related traits support the hypothesis of enhanced biochemical acclimation mechanisms activated under stress. Conversely, anatomical traits showed a more conservative response profile, with limited variation in key structural parameters such as palisade parenchyma thickness. The

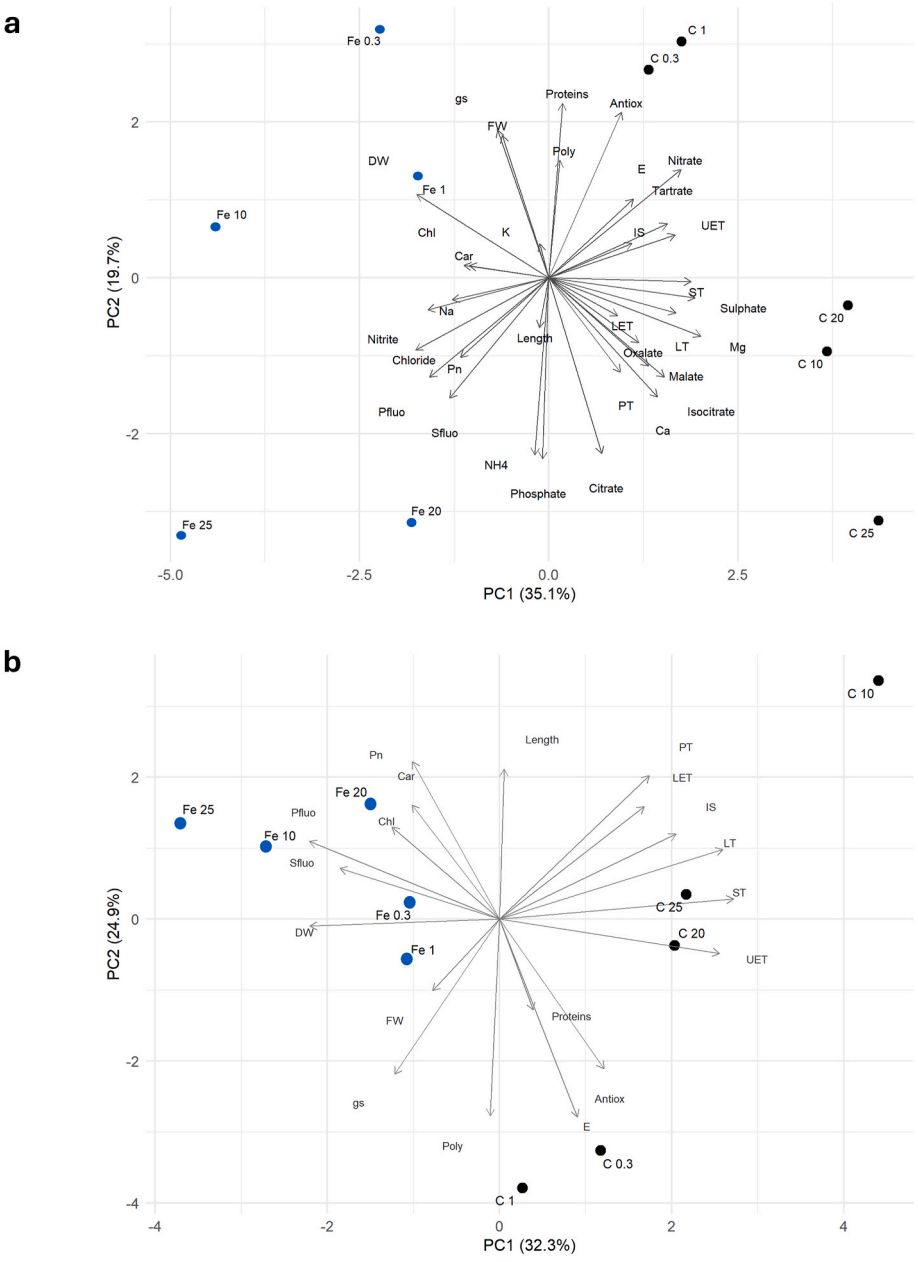

Fig. 5. Principal component analysis (PCA) loading plots and scores of (5a) all morphological (FW, fresh weight; DW, dry weight; microgreen length), anatomical (UET, upper epidermis thickness; PT, palisade parenchyma thickness; ST, spongy parenchyma thickness; LET, lower epidermis thickness; LT, total leaf lamina thickness; IS, intercellular space; PFluo, fluorescence intensity in palisade parenchyma; SFluo, fluorescence intensity in spongy parenchyma), ecophysiological (E, transpiration; gs, stomatal conductance; PN, net photosynthesis), and biochemical parameters (minerals: ammonium, nitrite, nitrate, sulfate, phosphate, sodium, potassium, magnesium, calcium, chloride; organic acids: oxalate, tartrate, malate, citrate, isocitrate; AC, antioxidant capacity; CHL, chlorophylls; CAR, carotenoids; POLY, polyphenols; PROT, soluble proteins), and (5b) the same dataset excluding minerals and organic acids, in *S. hispanica* microgreens from the control (0 Gy) and seedlings irradiated with increasing doses (0.3, 1, 10, 20, 25 Gy) of carbon and iron ions.

slightly higher plasticity of spongy tissue under iron-ion exposure suggests selective reorganization of leaf architecture, potentially enhancing gas diffusion and mitigating oxidative stress. These findings suggest that radiation quality could be strategically employed to modulate specific traits in microgreens, depending on the desired nutritional or physiological outcome. For instance, carbon ions may favor polyphenol accumulation, whereas iron ions may promote protein biosynthesis.

5. Conclusion

This study provides new insights into the effects of high-LET radiation on chia microgreens, highlighting their ion- and dose-specific physiological and biochemical acclimation. Fe-ion irradiation promoted structural growth and increased protein and pigment content, whereas C-ion exposure primarily affected traits related to water and nutrient dynamics, including transpiration, stomatal conductance, and mineral accumulation. Moderate doses induced hormetic responses, enhancing growth, while higher doses triggered metabolic and structural adjustments. Tissue-level responses contributed to maintaining photosynthetic function, whereas biochemical traits exhibited targeted plasticity, particularly under iron irradiation. Overall, these results highlight *S. hispanica* microgreens as a promising candidate for controlled-environment agriculture, including potential applications in space farming and functional food production. They also provide a basis

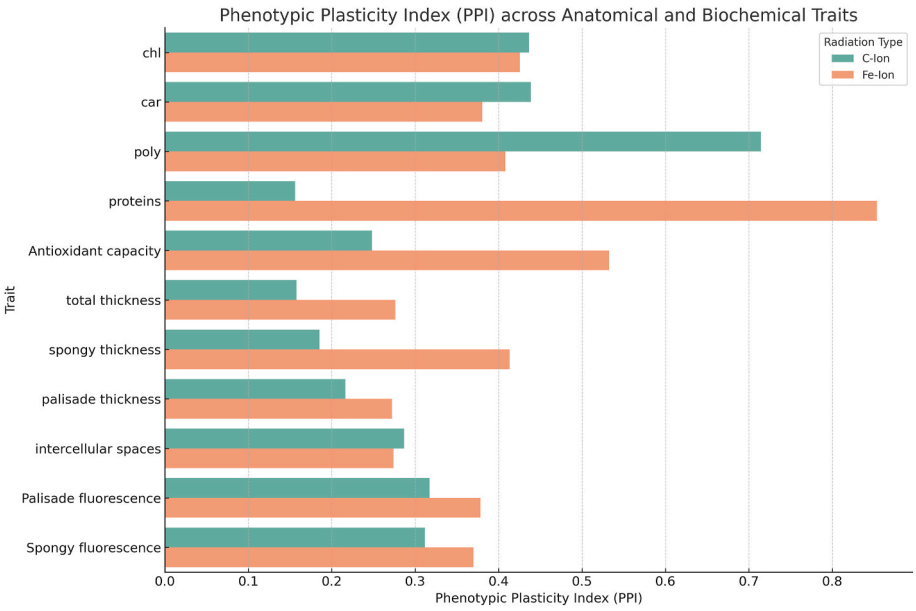

Fig. 6. Phenotypic Plasticity Index (PPI) of anatomical and biochemical traits in *S. hispanica* L. microgreens under C- and Fe-ion irradiation. Each bar represents the PPI calculated for a single trait across increasing radiation doses (0.3–25 Gy), with values ranging from 0 (no variation) to 1 (maximum variation). Biochemical traits (e.g., proteins, polyphenols, antioxidant capacity) showed higher plasticity than anatomical traits, particularly under Fe-ion exposure. This suggests a greater metabolic responsiveness to high-LET radiation. Data supporting this figure is provided in Table S1.

for future research aimed at optimizing crop performance under space-relevant radiation conditions, particularly in relation to nutritional quality and stress resilience. While the present study focuses on early developmental stages under controlled conditions, further research is warranted to assess long-term plant responses, yield performance, and the combined effects of multiple space-related stressors.

Funding

Open access funding provided by Università degli Studi di Napoli Federico II within the CRUI-CARE Agreement. The work was also partially carried out within the Space It Up! project funded by the Italian Space Agency, ASI, and the Ministry of University and Research, MUR, under contract n. 2024-5-E.0-CUP n. I53D24000060005. Part of the results presented here is based on the experiment Bio_08_DeMicco, which was performed at the SIS18 at the GSI Helmholtzzentrum fuer Schwerionenforschung, Darmstadt (Germany) in the frame of FAIR Phase-0.

CRediT authorship contribution statement

Sara De Francesco: Conceptualization, Data curation, Formal analysis, Investigation, Methodology, Writing – original draft, Writing – review & editing. **Chiara Amitrano:** Data curation, Formal analysis, Investigation, Methodology, Writing – review & editing. **Ermenegilda Vitale:** Formal analysis, Investigation, Methodology, Writing – review & editing. **Walter Tinganelli:** Investigation, Methodology, Writing – review & editing. **Marco Durante:** Methodology, Supervision, Writing – review & editing. **Stefania De Pascale:** Funding acquisition, Project administration, Supervision, Writing – review & editing. **Carmen Arena:** Conceptualization, Methodology, Resources, Supervision, Validation, Writing – review & editing. **Veronica De Micco:** Conceptualization, Data curation, Formal analysis, Funding acquisition, Investigation, Methodology, Project administration, Resources, Supervision, Validation, Writing – review & editing.

Declaration of competing interest

The authors declare that they have no known competing financial interests or personal relationships that could have appeared to influence the work reported in this paper.

Acknowledgements

The work by S.D.F. was supported by the European Space Agency and the Italian Space Agency within the MELiSSA (Micro-Ecological Life Support System Alternative) PhD POMP program with the project 'Radiation effect on plants' at the University of Naples PhD Sustainable Agricultural and Forestry Systems and Food Security (XXXVII Cycle).

Appendix A. Supplementary data

Supplementary data to this article can be found online at https://doi.org/10.1016/j.plaphy.2026.111517.

Data availability

Data will be made available on request.

References

Al-Younis, Z.K., Al-Shawi, S.G., Kareem, A.K., Rab, S.O., Jyothi, S.R., Mishra, S., et al., 2025. A critical review of the health benefits associated with chia seeds (*Salvia hispanica* L.). Plant Foods Hum. Nutr. 80, 170. https://doi.org/10.1007/s11130-025-01401-z.

Amitrano, C., Arena, C., De Pascale, S., Pugliese, M., Barozzi, F., Fanizzi, F.P., De Micco, V., Di Sansebastiano, G.P., 2025. Aquatic bryophytes as biofilters and resource regenerators in bioregenerative life support systems: the moss on Mars project. Front. Plant Sci. 16, 1667463. https://doi.org/10.3389/fpls.2025.1667463.

Amitrano, C., De Francesco, S., Durante, M., Tinganelli, W., Arena, C., De Micco, V., 2024. Morphological and photosynthetic pigment screening of four microgreens species exposed to heavy ions. Plants 13, 3541. https://doi.org/10.3390/plants13243541.

Amitrano, C., Junker, A., D'Agostino, N., De Pascale, S., De Micco, V., 2022. Integration of high-throughput phenotyping with anatomical traits of leaves to help understanding lettuce acclimation to a changing environment. Planta 256, 68. https://doi.org/10.1007/s00425-022-03984-2.

Amitrano, C., Paglialunga, G., Battistelli, A., De Micco, V., Del Bianco, M., Liuzzi, G., Moscatello, S., Paradiso, R., Proietti, S., Rouphael, Y., De Pascale, S., 2023. Defining

growth requirements of microgreens in space cultivation via biomass production, morpho-anatomical and nutritional traits analysis. Front. Plant Sci. 14, 1190945. https://doi.org/10.3389/fpls.2023.11909451.

Amitrano, C., Tinganelli, W., De Francesco, S., Durante, M., De Pascale, S., De Micco, V., 2026. Carbon-ion irradiation modulates early development of lettuce seedlings: a morphotype-specific response. Horticulturae 12, 614. https://doi.org/10.3390/horticulturae12050614.

Arena, C., Vitale, E., Hay Mele, B., Cataletto, P.R., Turano, M., Simoniello, P., De Micco, V., 2019. Suitability of *Solanum lycopersicum* L. 'Microtom' for growth in bioregenerative life support systems: exploring the effect of high-LET ionising radiation on photosynthesis, leaf structure and fruit traits. Plant Biol. 21, 615–626. https://doi.org/10.1111/plb.12952.

Biswas, S., Islam, F., Imran, A., Zahoor, T., Noreen, R., Fatima, M., Zahra, S.M., Asif Shah, M., 2023. Phytochemical profile, nutritional composition, and therapeutic potentials of chia seeds: a concise review. Cogent Food Agric. 9, 2220516. https://doi.org/10.1080/23311932.2023.2220516.

Borrelli, A., Zamani, F., Logegaray, V.R., Sanchez, E.C., Maseda, F.A., Alonso Quintas, J. M.C.J., Paradiso, R., 2026. Manipulation of light intensity and spectrum for driving growth and metabolism to improve nutritional and nutraceutical quality of microgreens. Plant Growth Regul. 106, 26. https://doi.org/10.1007/s10725-026-01434-7.

Bradford, M.M., 1976. A rapid and sensitive method for the quantitation of microgram quantities of protein utilizing the principle of protein-dye binding. Anal. Biochem. 72, 248–254. https://doi.org/10.1016/0003-2697(76)90527-3.

Cai, X., Huq, E., 2025. Shining light on plant growth: recent insights into phytochrome-interacting factors. J. Exp. Bot. 76 (3), 646–663. https://doi.org/10.1093/jxb/erae276.

De Falco, B., Amato, M., Lanzotti, V., 2017. Chia seeds products: an overview. Phytochem. Rev. 16, 745–760. https://doi.org/10.1007/s11101-017-9511-7.

De Francesco, S., Amitrano, C., Vitale, E., Costanzo, G., Pugliese, M., Arrichiello, C., et al., 2023. Growth, anatomical, and biochemical responses of the space farming candidate Brassica rapa L. microgreens to low-LET ionizing radiation. Horticulturae 9 (4), 452. https://doi.org/10.3390/horticulturae9040452.

De Francesco, S., Amitrano, C., Vitale, E., Costanzo, G., Tinganelli, W., Pugliese, M., Arrichiello, C., Muto, P., Durante, M., De Pascale, S., Arena, C., De Micco, V., 2025. Radiation quality matters: morphological and biochemical responses of Brassica rapa microgreens to X-rays, C-ions, and Fe-ions. Planta 262 (5), 118. https://doi.org/10.1007/s00425-025-04835-6.

De Micco, V., Amitrano, C., Mastroleo, F., Aronne, G., Battistelli, A., Carnero-Diaz, E., et al., 2023b. Plant and microbial science and technology as cornerstones to bioregenerative life support systems in space. npj Microgravity 9, 69. https://doi.org/10.1038/s41526-023-00317-9.

De Micco, V., Amitrano, C., Stinca, A., Izzo, L.G., Zalloni, E., Balzano, A., et al., 2020. Dust accumulation due to anthropogenic impact induces anatomical and photochemical changes in leaves of Centranthus ruber growing on the slope of the vesuvius volcano. Plant Biol. 22, 93–102 (DOI non fornito; aggiungi se disponibile).

De Micco, V., Arena, C., Aronne, G., 2014. Anatomical alterations of Phaseolus vulgaris L. mature leaves irradiated with X-rays. Plant Biol. 16, 187–193. https://doi.org/10.1111/plb.12125.

De Micco, V., Arena, C., Di Fino, L., Narici, L., 2022. Radiation environment in exploration-class space missions and plants' responses relevant for cultivation in bioregenerative life support systems. Front. Plant Sci. 13, 1001158. https://doi.org/10.3389/fpls.2022.1001158.

De Micco, V., Aronne, G., Caplin, N., Carnero-Diaz, E., Herranz, R., Horemans, N., et al., 2023a. Perspectives for plant biology in space and analogue environments. npj Microgravity 9, 67. https://doi.org/10.1038/s41526-023-00315-x.

Douglas, G.L., Cooper, M., Bermudez-Aguirre, D., Sirmons, T., 2016. Risk of performance decrement and crew illness due to an inadequate food system. NASA Johnson Space Center 1–47. Houston, TX, Report No. JSC-CN-37577.

Dubey, R.S., Srivastava, R.K., Pessarakli, M., 2021. Physiological mechanisms of nitrogen absorption and assimilation in plants under stressful conditions. In: Pessarakli, M. (Ed.), Handbook of Plant and Crop Physiology, fourth ed. CRC Press, Boca Raton, pp. 579–616.

Feder, N., O'Brien, T.P., 1968. Plant microtechnique: some principles and new methods. Am. J. Bot. 55, 123–142. https://doi.org/10.1002/j.1537-2197.1968.tb06952.x.

Ferreira, S.S., Antunes, M.S., 2021. Re-engineering plant phenylpropanoid metabolism with the aid of synthetic biosensors. Front. Plant Sci. 12, 701385. https://doi.org/10.3389/fpls.2021.701385.

Fukuzawa, K., Fujii, T., 1992. Peroxide-dependent and independent lipid peroxidation: site-specific mechanisms of initiation by chelated iron and inhibition by α-tocopherol. Lipids 27 (3), 227–233. https://doi.org/10.1007/BF02536187.

Huang, M., Xu, H., Zhou, Q., Xiao, J., Su, Y., Wang, M., 2025. The nutritional profile of chia seeds and sprouts: tailoring germination practices for enhancing health benefits—a comprehensive review. Crit. Rev. Food Sci. Nutr. 65 (12), 2365–2387. https://doi.org/10.1080/10408398.2024.2311873.

Im, J., Ko, J., Kim, H.Y., Ha, B.K., 2017. Biochemical responses of soybean (Glycine max L. Merr.) to proton beam irradiation. Plant Breed. Biotechnol. 5 (2), 97–105. https://doi.org/10.9787/PBB.2017.5.2.97.

Kyriacou, M.C., De Pascale, S., Kyratzis, A., Rouphael, Y., 2017. Microgreens as a component of space life support systems: a cornucopia of functional food. Front. Plant Sci. 8, 1587. https://doi.org/10.3389/fpls.2017.01587.

Li, P., Liu, C., Luo, Y., Shi, H., Li, Q., PinChu, C., et al., 2022. Oxalate in plants: metabolism, function, regulation, and application. J. Agric. Food Chem. 70 (51), 16037–16049. https://doi.org/10.1021/acs.jafc.2c05665.

Lichtenthaler, H.K., 1987. Chlorophylls and carotenoids: pigments of photosynthetic biomembranes. Methods Enzymol. 148, 350–382. https://doi.org/10.1016/0076-6879(87)48036-1.

Luoni, F., Weber, U., Boscolo, D., Durante, M., Reidel, C.A., Schuy, C., et al., 2020. Beam monitor calibration for radiobiological experiments with scanned high energy heavy ion beams at FAIR. Front. Phys. 8, 568145. https://doi.org/10.3389/fphy.2020.568145.

Motyka, S., Skała, E., Ekiert, H., Szopa, A., 2023. Health-promoting approaches of the use of chia seeds. J. Funct.Foods 103, 105480. https://doi.org/10.1016/j.jff.2023.105480.

Noblat, G.D.A., Souza, G.T., de Araújo, B.A.N., de Campos, L.M.T.D.S., Almeida, C., Figueiredo, M.S., 2025. *Salvia hispanica* L.: botanical characteristics, nutritional composition, and potential health benefits. Nutr. Rev. nuaf196. https://doi.org/10.1093/nutrit/nuaf196.

Rouphael, Y., Colla, G., Giordano, M., El-Nakhel, C., Kyriacou, M.C., De Pascale, S., 2017. Foliar applications of a legume-derived protein hydrolysate elicit dose-dependent increases of growth, leaf mineral composition, yield and fruit quality in two greenhouse tomato cultivars. Sci. Hortic. 226, 353–360. https://doi.org/10.1016/j.scienta.2017.09.003.

Ruzin, S.E., 2024. Techniques in Light Microscopy. Oxford University Press, Oxford.

Szopa, A., Motyka, S., Ekiert, H., 2023. Chia sprouts and microgreens as new nutraceutical raw materials and their health-promoting impact in modern dietetics. Curr. Issues Pharm. Med. Sci. 36 (1), 33–44. https://doi.org/10.2478/cipms-2023-0006.

Tariq, A., Zeng, F., Graciano, C., Ullah, A., Sadia, S., Ahmed, Z., et al., 2023. Regulation of metabolites by nutrients in plants. In: Plant Ionomics: Sensing, Signaling, and Regulation. Springer, pp. 1–18.

Teng, Z., Luo, Y., Pearlstein, D.J., Wheeler, R.M., Johnson, C.M., Wang, Q., Fonseca, J. M., 2023. Microgreens for home, commercial, and space farming: a comprehensive update of the most recent developments. Annu. Rev. Food Sci. Technol. 14, 539–562. https://doi.org/10.1146/annurev-food-060721-025930.

Valladares, F., Sanchez-Gomez, D., Zavala, M.A., 2006. Quantitative estimation of phenotypic plasticity: bridging the gap between the evolutionary concept and its ecological applications. J. Ecol. 94, 1103–1116. https://doi.org/10.1111/j.1365-2745.2006.01176.x.

Vitale, E., Izzo, L.G., Amitrano, C., Velikova, V., Tsonev, T., Simoniello, P., et al., 2022. Light quality modulates photosynthesis and antioxidant properties of Beta vulgaris L. plants from seeds irradiated with high-energy heavy ions: implications for cultivation in space. Plants 11 (14), 1816. https://doi.org/10.3390/plants11141816.

Vitale, E., Velikova, V., Tsonev, T., Ferrandino, I., Capriello, T., Arena, C., 2021b. The interplay between light quality and biostimulant application affects the antioxidant capacity and photosynthetic traits of soybean (Glycine max L. Merrill). Plants 10 (5), 861. https://doi.org/10.3390/plants10050861.

Vitale, E., Vitale, L., Costanzo, G., Velikova, V., Tsonev, T., Simoniello, P., et al., 2021a. Light spectral composition influences structural and eco-physiological traits of Solanum lycopersicum L. cv. 'Microtom' in response to high-LET ionizing radiation. Plants 10 (8), 1752. https://doi.org/10.3390/plants10081752.

Vitale, L., Vitale, E., Guercia, G., Turano, M., Arena, C., 2020. Effects of different light quality and biofertilizers on structural and physiological traits of spinach plants. Photosynthetica 58 (4), 932–943. https://doi.org/10.32615/ps.2020.041.

Volkova, P.Y., Bondarenko, E.V., Kazakova, E.A., 2022. Radiation hormesis in plants. Curr. Opin Toxicol. 30, 100334. https://doi.org/10.1016/j.cotox.2022.100334.

Weir, T.L., Bais, H.P., Stull, V.J., Callaway, R.M., Thelen, G.C., Ridenour, W.M., et al., 2006. Oxalate contributes to the resistance of Gaillardia grandiflora and Lupinus sericeus to a phytotoxin produced by Centaurea maculosa. Planta 223, 785–795. https://doi.org/10.1007/s00425-005-0130-2.